Double-slot Hybrid Plasmonic Cavity Used for Phase Modulation and Sensing

Xu Sun and Lech Wosinski
Laboratory of Photonics and Microwave Engineering, Royal Institute of Technology (KTH), Electrum 229, 164 40 Kista, Sweden.
xus@kth.se

Abstract: Highly-efficient double-slot hybrid plasmonic cavity is demonstrated. By measuring phase change with different liquids, we show that this sub-wavelength structure has better modulation efficiency than Si-based one for applications in ultra-compact highly-efficient sensors and modulators.

OCIS codes: (250.5403) plasmonics; (250.5300) Photonic integrated circuits; (040.6040) silicon.

1. Introduction

Hybrid plasmonic (HP) waveguides [1] allow for sub-wavelength confinement of guiding light with relatively low losses due to mixed photonic and plasmonic modes giving a flexible trade-off in the design between confinement and propagation length. This kind of structure attracted a lot of attention for realization of very compact photonic devices with subwavelength dimensions. A number of different disk-, ring- and donut resonators for different applications with sub-micron sizes have been designed and fabricated [2-4]. In this paper we present a double-slot hybrid plasmonic (HP) waveguide structure in application to sensing and modulation by measuring the phase shift of the Mach-Zehnder interferometer caused by liquid infiltration of one of the arms (the double-slot hybrid plasmonic waveguide).

2. Schematic and Numerical analysis

The schematic of the double-slot HP waveguide is shown in Fig. 1(a). A Si nanowire is located in the middle of the slot of plasmonic MIM (metal-insulator-metal) waveguide (we use silver as the metal material in this paper). Two narrow slots between silver pads and silicon nanowire are forming hybrid plasmonic waveguides and lead to a large optical confinement, which is similar to other kinds of HP waveguide structures. The height of silver pads is equal to the height of the Si nanowire, and the substrate is SiO_2 with infinite thickness (buffer layer). In our simulation, we set the refractive index of Si as 3.478, and the slot material (same as surrounding material) is assumed to be 1.35. The permittivity of silver is calculated by Durde model [5]:

$$\varepsilon_r = \varepsilon_\infty - \frac{\omega_p^2}{\omega^2 + j\gamma\omega}, \tag{1}$$

where $\varepsilon_\infty = 3.1$, $\omega_p = 140 \times 10^{14} rad/s$ and $\gamma = 0.31 \times 10^{14} rad/s$. The operation wavelength is 1550nm. The simulation is achieved by commercial finite-element-method using COMSOL Multiphysics software.

The inset Fig. 1(a) shows the electric field (Ex) distribution at the cross-section of the waveguide structure. The width of Si nanowire is 400nm, while the width of each slot is 200nm. One can see that relative large part of E-field is confined in the slot, which indicates the potential to gain a large phase change by adjusting the surrounding material properties.

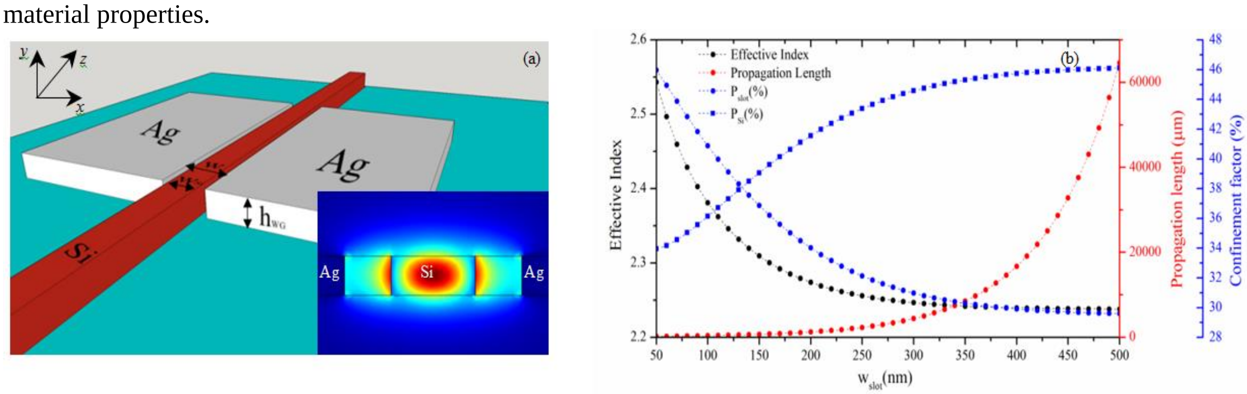

Figure 1: (a) Schematic and field distribution (inset) of double-slot HP waveguide. (b) Effective refractive index, propagation length and confinement factor changed with the width of slot.

By fixing the width and the height of Si nanowire to be 350nm and 250nm, the effective refractive index (N_{eff}), propagation length ($L_{prop} = \lambda_0/[2\pi \text{Im}(N_{eff})]$) and confinement factor (the power confined in Si or slot compared with the total power) as a function of the slot width have been illustrated in Fig. 1(b). The black and red curves represent the effective index and propagation length respectively. The blue curve with circles is the confinement factor of the slot, while the blue squares show confinement factor of Si. When the width of the slot increases, the propagation length increases too (the propagation loss decreases correspondingly), and the confinement factor of the slot decreases from 46% at 50nm to 30% at 500nm of the slot width. One should notice that the HP waveguide tends to Si wire with wide slot. From this figure, one can see that the HP waveguide acts similarly to Si nanowire when the width of the slot is larger than 500nm, where the propagation loss is as small as for the Si nanowire. That is due to decreasing contribution of plasmonics mode (photonics mode is dominant) with increasing width of the slots. However, the confinement factor of the slot (blue curve with circles) becomes smaller with wider width, which indicates that the modulation efficiency decreases. To study the trade-off between propagation loss and modulation efficiency, we can set $q = w_{Si}/w_{total}$ as a parameter. When q is equal to 0 or 1, the HP waveguide becomes a pure slot plasmonic waveguide.

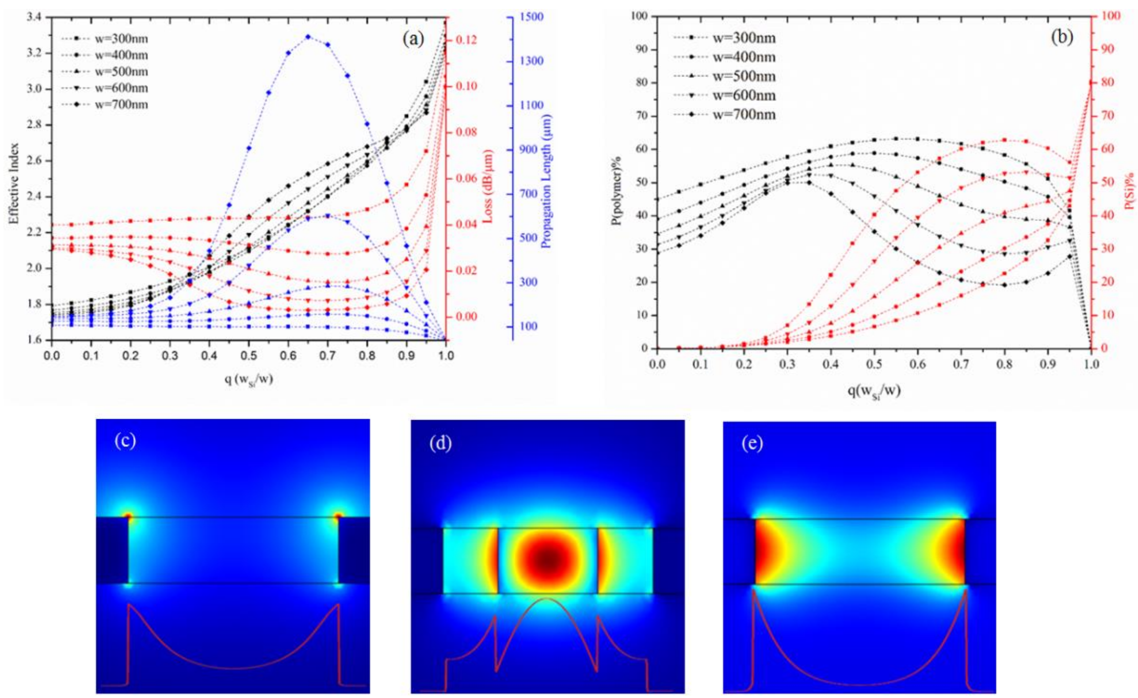

Figure 2: (a) Effective index, loss and propagation length changed with q, and (b) confinement factor of slot of Si changed with *q*. The total width is a parameter, increasing from 300nm to 700nm. (c), (d) and (e) are the E-field distributions when *q* is equal to 0, 0.5 and 1, respectively.

From the curves of propagation length (blue curves in Fig. 2 (a)) and confinement factor of the slot (red curves in Fig.2 (b)), one can notice the two advantages of double-slot HP waveguide compared with pure plasmonic slot waveguide: lower propagation loss (peak of propagation length) and larger modulation efficient (peak of confinement factor of the slots).

3. Experimental results

To measure the phase change of a double-slot HP waveguide, a design of Mach-Zehnder interferometer (MZI) is illustrated in Fig. 3(a). In order to get a high extinction ratio, the power difference between the double HP waveguide arm and reference arm should be small. The asymmetric design of MZI can decrease the power difference in some degree. Highly efficient non-uniform gratings [6] (not shown in this paper) are imprinted at the device ends to couple optical wave into and out of the devices.

The fabrication process started from commercial Silicon-on-insulator (SOI) wafer (250nm crystalline Silicon on top). After patterning the Si nanowire with e-beam lithography (EBL), dry etching of Si followed. Then, second time E-beam exposure and etch process was induced to fabricate the highly efficient grating couplers. Finally, the pattern of silver pads has been made by the third time EBL process. Metal lift-off process was then used to open the silver pads. The SEM figure of double-slot HP waveguide is shown in Fig. 3(b).

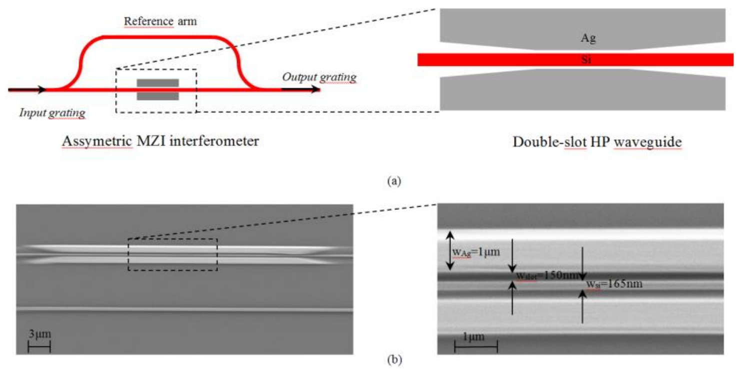

Figure 3: (a) Asymmetric Mach-Zehnder interferometer design for the phase change measurement. (b) SEM image of MZI interferometer and double-slot HP waveguide.

Different contents of isopropyl alcohol (IPA) in water were used to measure the modulation efficiency. After the optimization of modulation efficiency and loss by simulation as discussed above, we has fabricated the double-slot HP waveguide with the geometric parameters: w_{Si}=165nm and w_{slot}=150nm (N_{eff}=1.644-0.001314i). From the calculation, within the refractive index change between water and 100% IPA (~0.03), the π-length is only 40μm.

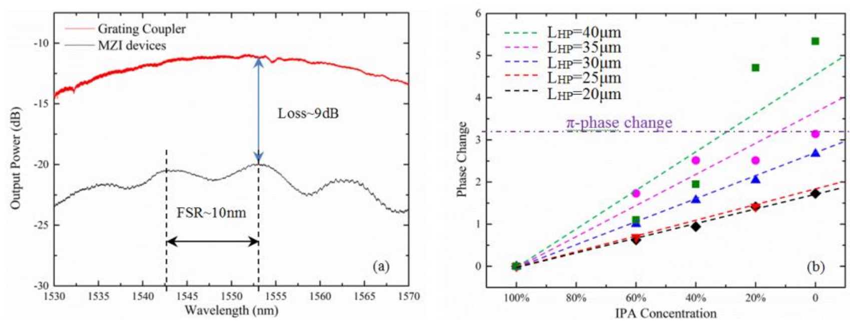

Figure 4: (a) Output spectrum of grating coupler and MZI. The insertion loss is about 9dB. (b) Phase changes of different lengths of double-slot HP waveguide from 100% IPA in water.

Fig. 4(a) shows the output spectrum of grating coupler and MZI, the insertion loss is about 9dB, which is reasonable due to the waveguide loss and fabrication loss. The large loss of double-slot HP waveguide arm makes the big power difference compared with the reference arm, which results in the low extinction ratio of MZI spectrum. Fig. 4(b) shows the phase change of different double-slot HP lengths (20μm to 40μm) from 100% IPA in water. One can see that with a longer double-slot HP waveguide, the sensor is more efficient. The π-phase change is less than 35μm, which agrees well with our calculation.

4. Conclusions

In conclusion, the benefits of double-slot HP waveguide at the aspects of propagation loss and modulation efficiency lead to the possibility of fabrication ultra-compact high-efficient phase sensitive devices that can be used as bio-sensors (filled with test liquids) and modulators (filled with non-linear active material).

5. Acknowledgment

This work was supported by "the Swedish Research Council (VR) through its Linnæus Center of Excellence ADOPT", as well as project VR-621-2010-4379.

6. References

[1] R.F. Oulton, V.J. Sorger, D.A. Genov, D.F.P. Pile, and X. Zhang, "A hybrid plasmonic waveguide for subwavelength confinement and long-range propagation," Nat. Photonics 2(8), p. 496 (2008).
[2] D. Dai, Y. Shi, S. He, L. Wosinski and L. Thylen, "Silicon hybrid plasmonic submicron-donut resonator with pure dielectric access waveguides", Optics Express, Vol. 19, No. 24, pp. 23671-23682 (2011).
[3] F. Lou, D. Dai, L. Thylen and L. Wosinski, "Design and analysis of ultra-compact EO polymer modulators based on hybrid plasmonic microring resonators", Opt. Express 21, 20041-20051 (2013).
[4] F. Lou, L. Thylen and L. Wosinski, "Ultra-sharp Bends Based on Hybrid Plasmonic Waveguides", 40th European Conference on Optical Communications (ECOC), Sep. 21-25, 2014, Cannes, France.
[5] C. Bohren and D. Huffman, *Absorption and Scattering of Light by Small Particle* (Wiley, 1983), Chap. 9.
[6] Y. Tang, Z. Wang, L. Wosinski, U. Westergren, and S. He, "Highly efficient nonuniform grating coupler for silicon-on-insulator nanophotonic circuits", Optics Letters, Vol. 35, Issue 8, pp.1290-1292 (2010).